

MEASUREMENT OF THE ELECTRON SPECTRUM FROM MUON DECAY,  
AND ITS IMPLICATIONS\*

R. D. Ehrlich, D. Fryberger,† R. J. Powers,‡ B. A. Sherwood,§ and V. L. Telegdi

Department of Physics and the Enrico Fermi Institute for Nuclear Studies,  
The University of Chicago, Chicago, Illinois

and

J. Bounin

Institute for Computer Research, University of Chicago, Chicago, Illinois  
(Received 6 January 1966)

The electron spectrum from muon decay, generally characterized (for unpolarized muons) by the two shape parameters  $\rho$  and  $\eta$  of Michel,<sup>1</sup> is of great theoretical interest. Regrettably, few of the experimental  $\rho$  values can claim high accuracy,<sup>2</sup> and some of these disagree with each other; furthermore, in interpreting their data, the authors generally assumed that which one hopes to check—namely, that the  $V-A$  interaction holds. No direct determination of  $\eta$  has been reported.<sup>3</sup>

This Letter has two goals: (a) to describe an accurate measurement, by a novel technique,<sup>4</sup> of the spectrum in question, including a determination of  $\eta$ ; (b) to discuss the interpretation, as regards the validity of the  $V-A$  theory, of this and kindred experiments.

We measure the momenta of the decay positrons in a homogeneous field, delineating their helical trajectories by means of seven wire spark chambers with magnetic core readout<sup>5</sup> (four for radius and three for pitch determination), placed within a magnet as shown in Fig. 1(a).

The following are some of the salient features of this nonfocusing spectrometer: (1) avoidance of wall and slit scattering; (2) large momentum acceptance ( $\Delta p \approx 30\%$ ) at a fixed, homogeneous field; (3) virtually momentum-independent solid angle within  $\Delta p$ ; (4) fair momentum resolution ( $dp/p \approx 1\%$ ); (5) positive identification of the  $\pi-\mu-e$  decay chain in the source; (6) ready adaptability to the measurement of the positron spectrum for polarized muons [with obvious changes in (4)].

Features (1) and (2) are improvements with respect to the classical spectrometers used in this field, but are shared by Columbia's sonic spark chamber apparatus.<sup>6</sup> The latter achieves (3) by different means, and is superior as regards (4). Feature (6) was the prime motivation for our geometry.

The source of our spectrometer is a  $\frac{1}{8}$ -inch

scintillator [counter 3 in Fig. 1(a)] in which pions injected through the coils are brought to rest. An acceptable positron produces a coincidence between 3 (anode) and two counters, 4 and 5, located behind the last wire chamber, in anticoincidence with two beam counters (1, 2) placed outside the magnet. Two pulses in counter 3 (dynode), separated by an interval of 7 to 80 nsec, generate after 100 nsec a 5- $\mu$ sec long gate through which a  $\bar{1}2345$  coincidence must pass to constitute a "real" event; this assures feature (5) mentioned above. Similarly, the  $\pi-\mu$  chain generates an identical gate delayed by 17  $\mu$ sec; events passing this latter gate are accidentals. Both "real" and accidental events trigger the chambers and initiate readout of the core arrays. The stored

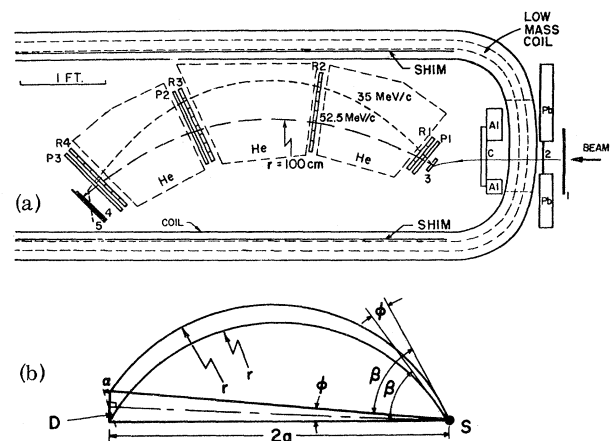


FIG. 1. (a) Experimental arrangement. R1 through R4 and P1 through P3 are wire spark chambers. The magnet is totally enclosed, and provides over most of the region of interest a field homogeneous to  $\leq 0.005\%$ . The He-filled boxes have  $5 \times 10^{-4}$ -in. Mylar windows. (b) Geometrical construction to compute the solid angle  $\Omega$  subtended by a plane in a magnetic field. One finds  $\Omega(t=r/a) \propto (t \arcsin t^{-1})^{-1} \times [1 + \tan \alpha (t^2 - 1)^{-1/2}]$ .

information is appropriately labeled, so that "real" and accidental spectra are collected at once. Under typical conditions, counter 3 was traversed by  $12 \times 10^3$  particles/sec and yielded  $10^3 \pi\text{-}\mu$  gates/sec, while the 12345 rate was 40/sec. The trigger rate was 1.4/sec.

Physically, each spark chamber in Fig. 1(a) consists of two "planes" of Al wires (0.1 mm diam) spaced 1 mm apart, yielding a resolution of  $\pm 0.32$  mm.<sup>4</sup> The equivalent thickness, including Mylar walls and Ne filling, is  $2 \times 10^{-4}$  radiation length. Spatial resolution and multiple scattering contribute here about equally to the uncertainty in determining the orbit radii, so that with a minimum sagitta of 50 mm one would have, for an ideal source,  $dp/p = \pm 0.8\%$ . Including energy losses in the source, one achieves an effective resolution of  $\pm 1\%$ .

The core arrays connected to the wire chambers were, of course, located outside the magnet. Their contents were either directly transmitted to a computer for on-line analysis,<sup>7</sup> or alternatively stored on magnetic tape.

**Selection criteria.**—Fig. 1(b) is the construction required to show that the solid angle  $\Omega(r)$  subtended by a small plane detector  $D$  at a point  $S$  is given by the expression in the caption. By choosing the angle  $\alpha$ , one can cancel the momentum (i.e.,  $r$ ) dependence to better than 0.1% over the  $\Delta p$  of interest; furthermore, this weak dependence is preserved for an ex-

tended source of the size used here. This is the basis of feature (3). In practice, the desired  $\alpha$  is not achieved through the actual positioning of counters 4 and 5, but rather by selection, in the data-analysis program, of orbits traversing an appropriate "virtual" detector. The illumination of the latter, as well as the source distribution, were also available from that program. The virtual detector was found to be uniformly illuminated.

Only those events (about  $10^6$ ) are analyzed which consist of a single spark in each chamber. The momentum is determined by fitting a helix to all seven spark coordinates. This over-determined helix is compared with a trial helix defined by all but the two terminal chambers; this comparison furnishes a criterion to eliminate badly scattered events. Only 4% of all analyzed events were rejected on this criterion. A detailed investigation convinces us that the cutoff chosen was momentum independent.

**Backgrounds.**—With the logic requirements imposed, beam particles could contribute only as accidentals. Indeed, the "real" spectrum had a contamination of only  $5 \times 10^{-5}$  for  $p > 60$  MeV/c. The accidentals were due to decay  $e^+$  originating in various parts of the apparatus. They were low (<5%), and because of their known spectrum constituted no source of bias.

**Source effects.**—Energy losses in the source

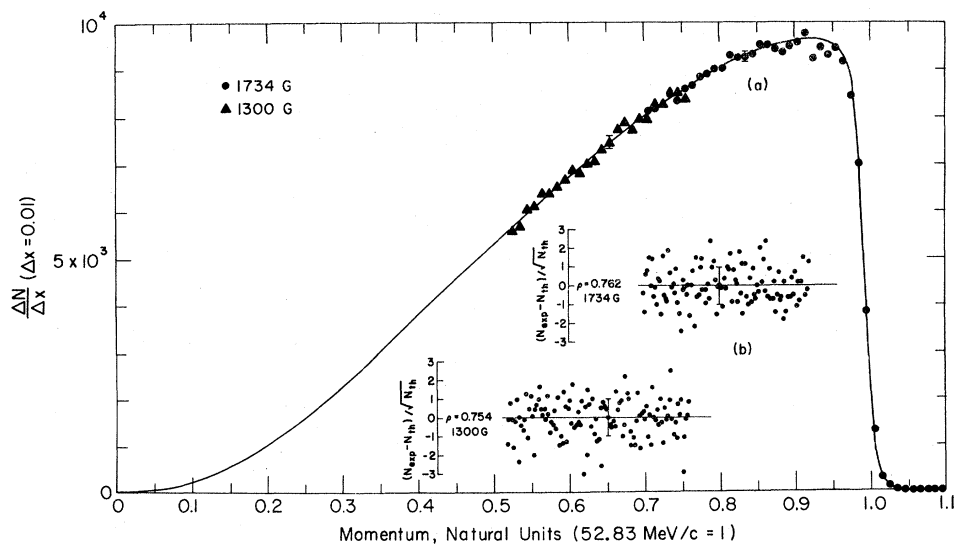


FIG. 2. (a) Experimental points. The points taken at 1300 G have been multiplied by a factor 2.19 for display. The solid line represents the Michel spectrum for  $\rho = 0.760$  and  $\eta \equiv 0$ , inclusive of radiative corrections,<sup>9</sup> with allowances for source losses and finite resolution. (b) Deviations of the experimental points from the best-fit theoretical curves, plotted in steps of 0.002 (natural momentum units).

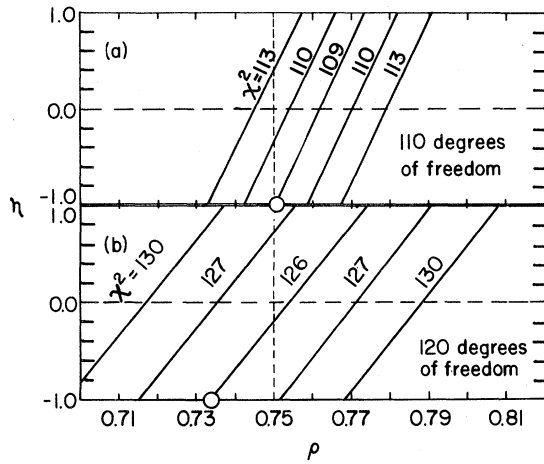


FIG. 3. Curves of constant  $\chi^2$  vs  $\rho$  and  $\eta$ ; these are portions of ellipses, approximated here by straight lines. The circles are the absolute minima of  $\chi^2$  attained with the constraint  $|\eta| \leq 1$ . (a) 1734-G data, (b) 1300-G data.

(0.45 g/cm<sup>2</sup>, 10<sup>-2</sup> radiation lengths) affect both the resolution and the momentum scale. The relevant loss distribution was obtained from the data of Goldwasser, Mills, and Hanson,<sup>8</sup> allowing for large losses by collision (Landau and radiation (Bethe-Heitler). Delta rays traversing the first chamber together with the primary  $e^+$  lead to rejected two-spark events. This leads, however, to no  $p$ -dependent bias since the Bhabha cross section for producing  $\delta^+$ 's of the required momentum is  $p$ -independent. Annihilation in flight, while  $p$ -dependent, occurs with  $<10^{-3}$  probability. The fact that pions are stopped in the source, in conjunction with the rapid muon precession, ensures an unpolarized muon sample.

**Absolute momentum scale.**—A precise measurement of the end point was not among the goals of this experiment. Rather the observed "end point" was used to calibrate the momentum scale, allowing for the finite resolution and target losses. The predicted "end point"

agrees with experiment to within the error (0.15 MeV) caused by uncertainties in chamber location.

**Statistical analysis.**—The experimental spectra at the two most useful field settings (1734 and 1300 G) are shown in Fig. 2(a); after folding in the appropriate resolution function they are compared with the theoretical spectrum,<sup>9</sup> varying the parameters  $\rho$  and  $\eta$ , and recording the  $\chi^2$  values. The dependence of  $\chi^2$  on  $\rho$  and  $\eta$  is shown in Fig. 3, and the best estimates of  $\rho$  and  $\eta$  ( $\chi^2$  minimum) are given in Table I. The curve in Fig. 2(a) represents the best fit; the deviations from it are shown in Fig. 2(b).

The analysis is insensitive to the intrinsic (massless source) resolution, provided that data near the end point are not used. Moreover this resolution (derived semiempirically) is, allowing for the source losses, in fair agreement with the edge of the spectrum. Only the radiative tail of these losses significantly influences the spectrum: Neglect of bremsstrahlung would decrease our  $\rho$  by 0.008. The errors in Table I include, in addition to the statistical errors, allowances for systematic errors in the effective radiative-source thickness, and in the absolute momentum scale. In fitting the data taken at a given field, variations in the boundaries of the momentum regions included and/or in the size of the virtual detector yielded statistically consistent values of  $\rho$  and  $\chi^2$ ; this supports our belief, based on independent estimates, that other systematic errors are negligible.

**Interpretation.**—The theory<sup>9</sup> underlying our fits assumes a lepton-conserving local interaction involving massless neutrinos. Within this framework, the observed parameters  $\rho$  and  $\eta$  serve (together with the other parameters of muon decay) to restrict the nature of the interaction. In particular, one would like to test the predictions of the  $V-A$  theory, which is a very special subcase. This theory predicts  $\rho = \frac{3}{4}$ , and until now—except for Plano's work<sup>3</sup>

Table I. Experimental results.

Magnetic field (G)	Momentum region <sup>a</sup>	Number of events	$\rho$ ( $\eta \equiv 0$ )	$\eta$ ( $\rho = \frac{3}{4}$ )	$\rho$ ( $ \eta  \leq 1$ )
1300	0.52-0.76	$80 \times 10^3$	$0.754 \pm 0.020$	$-0.2 \pm 1.0$	$0.733^{+0.060}_{-0.020}$
1734	0.70-0.92	$200 \times 10^3$	$0.762 \pm 0.010$	$-1.0 \pm 0.8$	$0.750^{+0.030}_{-0.010}$
Weighted average		$280 \times 10^3$	$0.760 \pm 0.009$	$-0.7 \pm 0.6$	$0.765^{+0.015}_{-0.028}$

<sup>a</sup>In natural momentum units.

Table II. Predicted muon decay parameters.

Theory	$\rho$	$\delta$	$\eta$	$\xi$	$h$
$V+\epsilon A$	$\frac{3}{4}$	$\frac{3}{4}$	$\frac{ \epsilon ^2-1}{2(1+ \epsilon ^2)}$	$\frac{-2\text{Re}(\epsilon)}{1+ \epsilon ^2}$	$=\xi$
$V-A$	$\frac{3}{4}$	$\frac{3}{4}$	0	1	1

—it has been traditional to fit the experimental spectra for  $\rho$  alone, ignoring the low-energy parameter  $\eta$  altogether (i.e., assuming  $\eta=0$ !).

On the other hand,  $\rho=\frac{3}{4}$  is not a very specific prediction of  $V-A$ . To illustrate this point, assume merely that neutrinos are two-component (with  $\nu=\nu_L$ ), leading automatically to a  $V+\epsilon A$  theory. Table II summarizes its predictions. One sees that  $\rho$  (and  $\delta$ ) do not restrict  $\epsilon$ , whereas  $\eta$  (and  $\xi$ ) do. Hence,  $\eta$  is the more relevant parameter in the spectrum from unpolarized muons.

In the tradition mentioned, our original goal was to measure  $\rho$  to the neglect of  $\eta$ . As was just emphasized, this is rather uninformative. Furthermore, even in that portion of the spectrum most sensitive to  $\rho$  and least sensitive to  $\eta$  (say,  $x>0.5$ ), the effect of  $\eta$  is large in a precision measurement, as Fig. 3 clearly shows. The information contained in this figure may be presented in different ways (see Table I): (a) fitted for  $\rho$ , constraining<sup>10</sup>  $|\eta|<1$  (our statistics being inadequate to fit for both  $\rho$  and  $\eta$ ); (b) fitted for  $\eta$ , with the  $V+\epsilon A$  constraint  $\rho=\frac{3}{4}$ , and (c) fitted for  $\rho$ , with  $\eta=0$ , as a comparison with other work. Our result (c) and that  $(\rho=0.747\pm 0.005)^2$  from the Columbia spectrometer agree, a fact which in view of the different sources of systematic error has more than statistical merit. In this regard, it is worth mentioning that the Columbia spectrum has, as compared to ours, three times as many events, but a worse fit ( $\chi^2 \approx 55$  for  $35 \pm 8.4$  expected).<sup>11</sup>

We thank K. Sebesta and R. W. Swanson for continued technical assistance, and T. A. Nunamaker for many contributions to the electronics. Finally, we are indebted to M. J. Neu-

mann and R. H. Hildebrand for enlightening discussions.

\*Research supported by U. S. Office of Naval Research, Contract No. Nonr 2121(25).

†Fellow, Fannie and John Hertz Foundation, 1964-66.

‡National Science Foundation Predoctoral Fellow, 1961-66.

§National Science Foundation Predoctoral Fellow, 1962-66; now at California Institute of Technology, Pasadena, California.

<sup>1</sup>L. Michel, Mém. Poudres Annexe 35, 77 (1953).

<sup>2</sup>The most accurate value of  $\rho$  is that of M. Bardon, P. Norton, J. Peoples, A. M. Sachs, and J. Lee-Franzini, Phys. Rev. Letters 14, 449 (1965). This paper lists some of the earlier values.

<sup>3</sup>R. J. Plano, Phys. Rev. 119, 1400 (1960), has attempted to measure  $\eta$ . See, however, the last paragraph on p. 1405 of his report.

<sup>4</sup>B. A. Sherwood, R. D. Ehrlich, D. Fryberger, R. J. Powers, V. L. Telegdi, and J. Bounin, post-deadline paper at the meeting of The American Physical Society, New York, January 1965 (unpublished); IEEE, Trans. Nucl. Sci. 12, No. 4 49 (1965).

<sup>5</sup>M. J. Neumann and H. Sherrard, IEEE, Trans. Nucl. Sci. 9, No. 3, 259 (1962); 9, No. 5, 58 (1962). For other references, see W. A. Higinbotham, IEEE, Trans. Nucl. Sci. 12, No. 4, 199 (1965).

<sup>6</sup>M. Bardon, J. Lee, P. Norton, J. Peoples, and A. M. Sachs, in Proceedings of the International Conference on Filmless Spark Chamber Techniques, Geneva, Switzerland, 1964, CERN Report No. 64-30, p. 41 (unpublished).

<sup>7</sup>MANIAC III of the University's Institute for Computer Research. We are greatly indebted to R. H. Miller and his staff for their untiring efforts.

<sup>8</sup>E. L. Goldwasser, F. E. Mills, and A. O. Hanson, Phys. Rev. 88, 1137 (1952).

<sup>9</sup>The theoretical spectrum, including radiative corrections for  $V$  and  $A$ , was taken from T. Kinoshita and A. Sirlin, Phys. Rev. 113, 1652 (1959). Instead of their  $\zeta$ , we use Michel's  $\eta=\zeta/2$ .

<sup>10</sup>This constraint, valid in the general theory, follows from the definition of  $\eta$ ; see C. Bouchiat and L. Michel, Phys. Rev. 106, 170 (1957). A stronger constraint  $\eta^2 \leq (1-\xi^2)/4$ , imposed by Plano in determining  $\rho$ , holds only for  $\rho=\frac{3}{4}$  ( $V+\epsilon A$ ). We thank Professor Plano for helpful correspondence.

<sup>11</sup>Since this Letter was written, we have learned that the Columbia group have reinvestigated their data, and now obtain an excellent  $\chi^2$  value. We are greatly indebted to Dr. A. M. Sachs for this information and helpful correspondence.